RESEARCH BRIEF

EGFR Kinase Domain Duplication (*EGFR*-KDD) Is a Novel Oncogenic Driver in Lung Cancer That Is Clinically Responsive to Afatinib

Jean-Nicolas Gallant[1,2], Jonathan H. Sheehan[3,4], Timothy M. Shaver[2,3], Mark Bailey[5], Doron Lipson[5], Raghu Chandramohan[6], Monica Red Brewer[2,7], Sally J. York[2,7], Mark G. Kris[8], Jennifer A. Pietenpol[2,3], Marc Ladanyi[6], Vincent A. Miller[5], Siraj M. Ali[5], Jens Meiler[4,9], and Christine M. Lovly[1,2,7]

ABSTRACT Oncogenic *EGFR* mutations are found in 10% to 35% of lung adenocarcinomas. Such mutations, which present most commonly as small in-frame deletions in exon 19 or point mutations in exon 21 (L858R), confer sensitivity to EGFR tyrosine kinase inhibitors (TKI). In analyzing the tumor from a 33-year-old male never-smoker, we identified a novel *EGFR* alteration in lung cancer: *EGFR* exon 18–25 kinase domain duplication (*EGFR*-KDD). Through analysis of a larger cohort of tumor samples, we detected additional cases of *EGFR*-KDD in lung, brain, and other cancers. *In vitro*, EGFR-KDD is constitutively active, and computational modeling provides potential mechanistic support for its auto-activation. *EGFR*-KDD–transformed cells are sensitive to EGFR TKIs and, consistent with these *in vitro* findings, the index patient had a partial response to the EGFR TKI afatinib. The patient eventually progressed, at which time resequencing revealed an EGFR-dependent mechanism of acquired resistance to afatinib, thereby validating *EGFR*-KDD as a driver alteration and therapeutic target.

SIGNIFICANCE: We identified oncogenic and drug-sensitive *EGFR*-KDD that is recurrent in lung, brain, and soft-tissue cancers and documented that a patient with metastatic lung adenocarcinoma harboring the *EGFR*-KDD derived significant antitumor response from treatment with the EGFR inhibitor afatinib. Findings from these studies will be immediately translatable, as there are already several approved EGFR inhibitors in clinical use. *Cancer Discov; 5(11); 1155–63. ©2015 AACR.*

INTRODUCTION

The prospective identification and rational therapeutic targeting of tumor genomic alterations have revolutionized the care of patients with lung cancer and other malignancies. Oncogenic mutations in the EGFR tyrosine kinase domain are found in an important subset of non–small cell lung cancer (NSCLC), and several large phase III clinical trials have shown that patients with *EGFR*-mutant lung cancer derive superior clinical responses when treated with EGFR tyrosine

[1]Department of Cancer Biology, Vanderbilt University Medical Center, Nashville, Tennessee. [2]Vanderbilt-Ingram Cancer Center, Vanderbilt University Medical Center, Nashville, Tennessee. [3]Department of Biochemistry, Vanderbilt University Medical Center, Nashville, Tennessee. [4]Center for Structural Biology, Vanderbilt University Medical Center, Nashville, Tennessee. [5]Foundation Medicine Inc., Cambridge, Massachusetts. [6]Department of Pathology, Memorial Sloan Kettering Cancer Center, New York, New York. [7]Department of Medicine, Vanderbilt University Medical Center, Nashville, Tennessee. [8]Department of Medicine, Memorial Sloan Kettering Cancer Center, New York, New York. [9]Department of Chemistry, Vanderbilt University Medical Center, Nashville, Tennessee.

Note: Supplementary data for this article are available at Cancer Discovery Online (http://cancerdiscovery.aacrjournals.org/).

Corresponding Author: Christine M. Lovly, Vanderbilt University Medical Center, 2220 Pierce Avenue, 777 Preston Research Building, Nashville, TN 37232. Phone 615-936-3457; Fax: 615-343-2973; E-mail: christine.lovly@vanderbilt.edu

doi: 10.1158/2159-8290.CD-15-0654

kinase inhibitors (TKI) as compared with standard chemotherapy (1–3). Such mutations, which most commonly occur as either small in-frame deletions in exon 19 or point mutations in exon 21 (L858R), confer constitutive activity to the EGFR tyrosine kinase and sensitivity to EGFR TKIs (4). Other oncogenic alterations, including *ALK* and *ROS1* gene rearrangements, have similarly allowed for the rational treatment of molecular cohorts of NSCLC. Unfortunately, despite these significant advances in defining clinically relevant molecular cohorts of lung cancer, the currently identified genomic alterations account for only 50% to 60% of all tumors. Additional analyses are necessary to identify therapeutically actionable molecular alterations in these tumors.

Here, we describe the case of a 33-year-old male never-smoker with metastatic lung adenocarcinoma whose tumor lacked all previously described actionable genomic alterations in this disease. Targeted next-generation sequencing (NGS)–based genomic profiling identified a novel in-frame tandem duplication of *EGFR* exons 18–25, the exons that encode the EGFR tyrosine kinase domain. This *EGFR* kinase domain duplication (*EGFR*-KDD) had not previously been reported in lung cancer, and there were no preclinical data or clinical evidence to support the use of EGFR inhibitors in patients whose tumors harbor the *EGFR*-KDD. However, the index patient was treated with the EGFR inhibitor afatinib, with rapid symptomatic improvement and significant decrease in tumor burden. Notably, upon disease progression, the patient's tumor harbored an increase in the copy number of the *EGFR*-KDD, solidifying the role of this *EGFR* alteration as a novel driver in this disease. Through analysis of a large set of annotated tumors, we demonstrate that the *EGFR*-KDD is recurrent in lung, brain, and soft-tissue tumors. Overall, our data show, for the first time, that *EGFR*-KDD is an oncogenic and therapeutically actionable alteration.

RESULTS

Case Report

A 33-year-old male never-smoker was diagnosed with stage IV lung adenocarcinoma after presenting with cough and fatigue. His tumor biopsy was sent for genomic profiling using an extensively validated hybrid-capture–based NGS diagnostic assay (FoundationOne; ref. 5). The patient's tumor was found to be negative for any previously described actionable alterations in lung cancer, including negative for the presence of previously described *EGFR* alterations, such as L858R, G719A/C/S, and L861Q point mutations, exon 19 deletion/insertion, and exon 20 insertion. Interestingly, however, the patient's tumor was found to harbor an intragenic alteration in *EGFR* resulting in the tandem duplication of exons 18 to 25 (Supplementary Fig. S1A). The presence of this alteration was confirmed by direct sequencing (data not shown) and by an independent clinical NGS assay (MSK-IMPACT; ref. 6; Supplementary Fig. S1B). Because exons 18 to 25 of *EGFR* encode the entire tyrosine kinase domain, this alteration results in an EGFR protein that has an in-frame kinase domain duplication (Fig. 1A and Supplementary Fig. S2). Notably, this *EGFR* alteration had not previously been reported in lung cancer; the *EGFR*-KDD (as duplication of exons 18–25 or 18–26) had been reported only in isolated cases of glioma to date (7–11). There were no data regarding the frequency of this alteration in tumor samples, nor were there data regarding the efficacy of EGFR-targeted agents against the *EGFR*-KDD.

Frequency of *EGFR*-KDD in Lung and Other Cancers

To determine the frequency of the *EGFR*-KDD in lung cancer and other tumors, we analyzed data from >38,000 clinical cases, each of which had results from FoundationOne targeted sequencing, analogous to the index patient. The *EGFR*-KDD was detected in 5 tumors from ~7,200 total lung cancers tested. In addition, *EGFR*-KDD was identified in 3 gliomas, 1 sarcoma, 1 peritoneal carcinoma, and 1 Wilms' Tumor (Table 1). Among samples in The Cancer Genome Atlas (TCGA), we found previously unreported cases of the *EGFR*-KDD in lung adenocarcinoma and glioblastoma multiforme (Table 1 and Supplementary Fig. S3A–S3D). Two additional cases were found by MSK-IMPACT sequencing (Table 1). Together, these data show that the *EGFR*-KDD is a recurrent mutation in lung cancer, glioma, and other human malignancies. It is important to note, however, that because most conventional (exomic) sequencing platforms would not routinely detect this particular *EGFR* alteration (due to its intronic breakpoints), these numbers are likely an underestimate, and the true prevalence of the *EGFR*-KDD remains unknown.

The *EGFR*-KDD Is Oncogenic

We expressed EGFR-KDD in NR6 and Ba/F3 cells (Fig. 1B–E). We observed expression of EGFR-KDD at the expected molecular weight as compared to EGFR wild-type ($EGFR^{WT}$) and the well-characterized $EGFR^{L858R}$ mutation (Fig. 1B and D). In contrast to $EGFR^{WT}$, both $EGFR^{L858R}$ and EGFR-KDD displayed high levels of autophosphorylation. Consistent with these data, EGFR-KDD protein is constitutively autophosphorylated in the absence of serum in A1235 cells, a glioma cell line which harbors endogenous EGFR-KDD (Supplementary Fig. S4; ref. 7). To address whether *EGFR*-KDD is an oncogenic alteration, we tested its ability to confer anchorage-independent growth to NR6 cells. EGFR-KDD significantly increased colony formation in soft agar as compared with both $EGFR^{WT}$ and the known oncogenic $EGFR^{L858R}$ mutation (Fig. 1C and Supplementary Fig. S5A–S5D). Expression of a kinase-dead version of the EGFR-KDD (called EGFR-KDD-dead) abrogated the growth of NR6 cells in soft agar, consistent with the requirement of kinase activity for anchorage-independent growth. In parallel, we expressed the same EGFR variants in Ba/F3 cells (Fig. 1D). EGFR-KDD, but not its kinase-dead counterpart, induced IL3-independent proliferation of Ba/F3 cells, an activity phenotype associated with the transforming function of other oncogenic tyrosine kinases (Fig. 1E; ref. 12). As previously reported, $EGFR^{L858R}$, but not $EGFR^{WT}$, was able to support IL3-independent growth of Ba/F3 cells (12).

Computational Modeling Demonstrates That EGFR-KDD Can Form Intramolecular Dimers

To provide insight into the mechanism of activation of EGFR-KDD, we examined the structure of the EGFR. The EGFR tyrosine kinase is known to be activated either due to increased local concentration of EGFR (e.g., as a result of

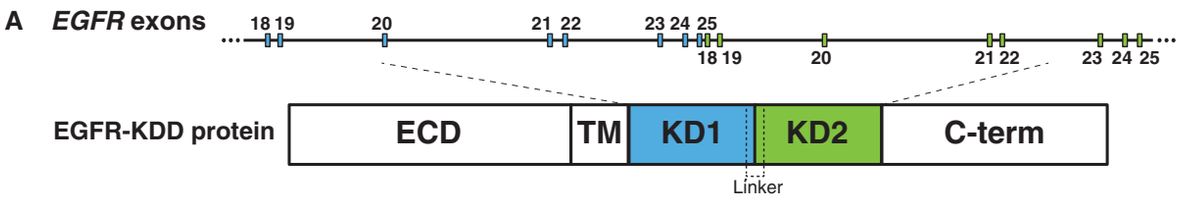

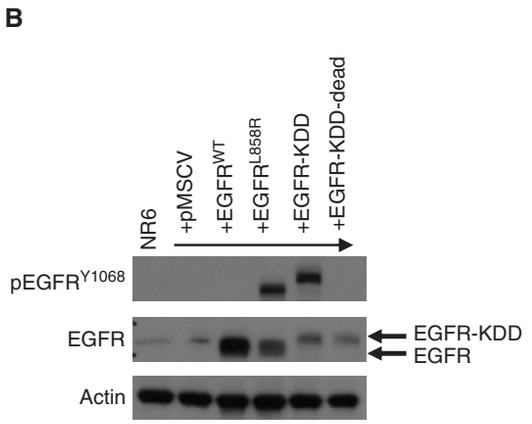

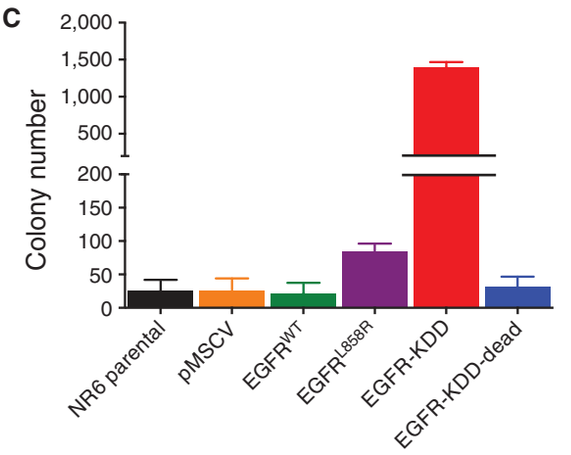

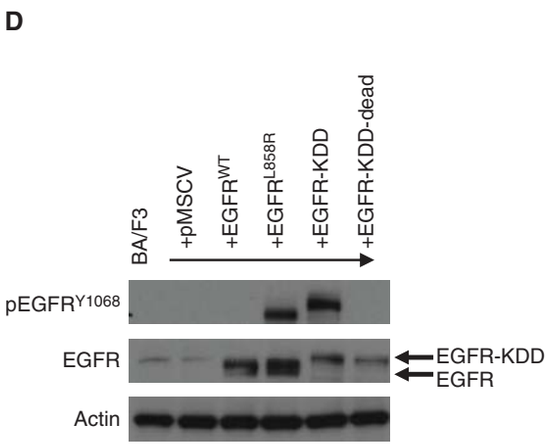

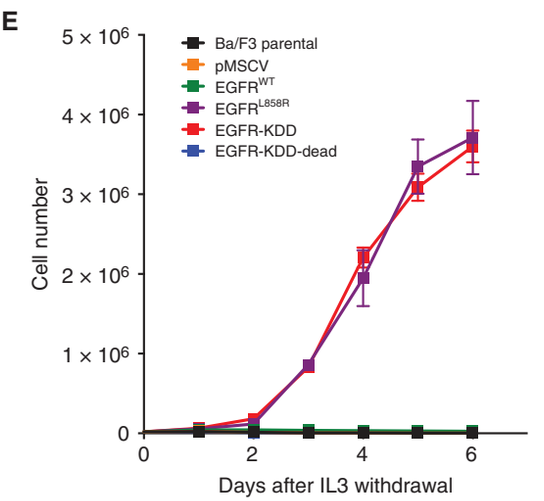

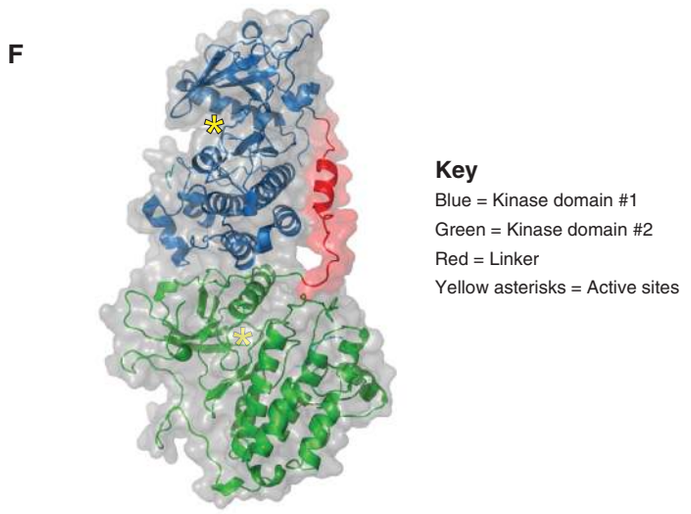

Figure 1. The *EGFR*-KDD is an oncogenic *EGFR* alteration. **A,** schematic representation of EGFR-KDD depicting the genetic and protein domain structures. ECD, extracellular domain; TM, transmembrane domain; KD1, first kinase domain; KD2, second kinase domain; C-term, carboxyl terminus. Blue, *EGFR* exons 18–25 #1; green, *EGFR* exons 18–25 #2. **B,** representative Western blot of NR6 cells stably expressing indicated EGFR constructs. EGFR-KDD-dead is a kinase-dead version of EGFR-KDD. **C,** NR6 cells stably expressing the indicated constructs (pMSCV = vector only) were plated in triplicate in soft agar, grown for 15 days, and quantified for colony formation. **D,** representative Western blot of BA/F3 cells expressing indicated EGFR constructs. **E,** BA/F3 cells transfected with indicated constructs (pMSCV = vector only) were grown in the absence of IL3 and counted every 24 hours. **F,** ribbon diagram and space-filling model of the EGFR-KDD kinase domains (GLY 696 - PRO 1370) illustrating the proposed mechanism of autoactivation.

Table 1. The *EGFR*-KDD is a recurrent alteration

Dataset	Identification #	Age	Gender	Reported diagnosis
Foundation Medicine	FM-1	52	Female	Lung adenocarcinoma
	FM-2[a]	33	Male	Lung adenocarcinoma
	FM-3	53	Female	Lung adenocarcinoma
	FM-4	57	Female	Lung adenocarcinoma
	FM-5	29	Female	Lung NSCLC (NOS)
	FM-6	53	Female	Brain astrocytoma
	FM-7	49	Male	Brain glioblastoma
	FM-8	54	Male	Brain glioblastoma
	FM-9	2	Female	Kidney Wilms' tumor
	FM-10	63	Female	Peritoneal serous carcinoma
	FM-11	27	Female	Soft tissue sarcoma (NOS)
TCGA	TCGA-49-4512	69	Male	Lung adenocarcinoma
	TCGA-12-0821	62	Female	Brain glioblastoma
MSKCC	MSKCC-1[a]	33	Male	Lung adenocarcinoma
	MSKCC-2	67	Female	Lung adenocarcinoma
	MSKCC-3[b]	53	Male	Brain glioblastoma

NOTE: Characteristics of *EGFR*-KDD exons 18–25 patients from Foundation Medicine, TCGA, and Memorial Sloan Kettering Cancer Center datasets.

Abbreviation: NOS, not otherwise specified.

[a], index patient; [b], this patient's tumor also contained high level amplification of $EGFR^{WT}$ and an $EGFR^{G719C}$ mutation. The *EGFR*-KDD and $EGFR^{G719C}$ alterations were below the level of $EGFR^{WT}$ amplification, and presumably reflect subclonal populations.

ligand binding or overexpression), mutations in the activation loop (e.g., L858R), or through formation of asymmetric (N-lobe to C-lobe) intermolecular dimers between two EGFR proteins (13). Given the presence of two tandem in-frame kinase domains within the EGFR-KDD structure, we hypothesized that EGFR-KDD could form an intramolecular dimer. To test this hypothesis, we modeled the EGFR-KDD based on the available experimental structure of the active asymmetric EGFR dimer (13). Conformational loop sampling with Rosetta demonstrates that the linker between the tandem tyrosine kinase domains allows for the proper positioning of the two domains necessary for asymmetric dimerization and intramolecular EGFR activation (Fig. 1F). Therefore, our model suggests that EGFR-KDD is an oncogenic variant of the EGFR likely by virtue of its ability to form intramolecular asymmetric activated dimers. Although modeling demonstrates that the EGFR-KDD is geometrically capable of forming intramolecular asymmetric dimers, further experimental data would be needed to confirm this mechanism.

The EGFR-KDD Can Be Therapeutically Targeted with Existing EGFR TKIs

We sought to determine whether EGFR TKIs are an effective therapeutic strategy for tumors harboring the EGFR-KDD. We treated Ba/F3 cells expressing $EGFR^{WT}$, $EGFR^{L858R}$, and EGFR-KDD with erlotinib (first-generation reversible EGFR TKI; ref. 14), afatinib (second-generation irreversible inhibitor of EGFR/HER2; ref. 15), and AZD9291 (third-generation mutant-specific EGFR TKI; ref. 16) to assess the effects of these inhibitors on the autophosphorylation (and by extension, the kinase activity) and downstream signaling properties of the EGFR kinase. All three EGFR TKIs were able to inhibit EGFR-KDD tyrosine phosphorylation in a dose-dependent manner, albeit to different levels (Fig. 2A). Afatinib was the most potent inhibitor of EGFR-KDD autophosphorylation, at doses similar to those required for $EGFR^{L858R}$ inhibition. Activation of downstream MAPK signaling was also inhibited in Ba/F3 cells expressing EGFR-KDD, as shown by decreased ERK phosphorylation after drug treatment. Similar results were observed in 293T cells transfected with EGFR variants (Supplementary Fig. S6A) and in A1235 cells which harbor endogenous EGFR-KDD (Supplementary Fig. S6B). To determine whether inhibition of EGFR autophosphorylation translated to inhibition of cellular proliferation, we treated Ba/F3 cells expressing various EGFR constructs with erlotinib, afatinib, and AZD9291. All three distinct EGFR TKIs effectively inhibited the growth of EGFR-KDD Ba/F3 cells (Fig. 2B and Supplementary Table S1). Consistent with our signaling data, the growth inhibition observed was most pronounced with afatinib. Analogous results were seen in A1235 cells (Supplementary Fig. S6C). Together, these results show that the EGFR-KDD can be potently inhibited by afatinib, leading to decreased cell viability.

Treatment of the Index Patient with Afatinib

Because there were no data regarding the use of EGFR TKIs or monoclonal antibodies in the setting of a tumor harboring the *EGFR*-KDD, the index patient was initially treated with standard first-line chemotherapy for stage IV lung adenocarcinoma (cisplatin/pemetrexed/bevacizumab). However, at the

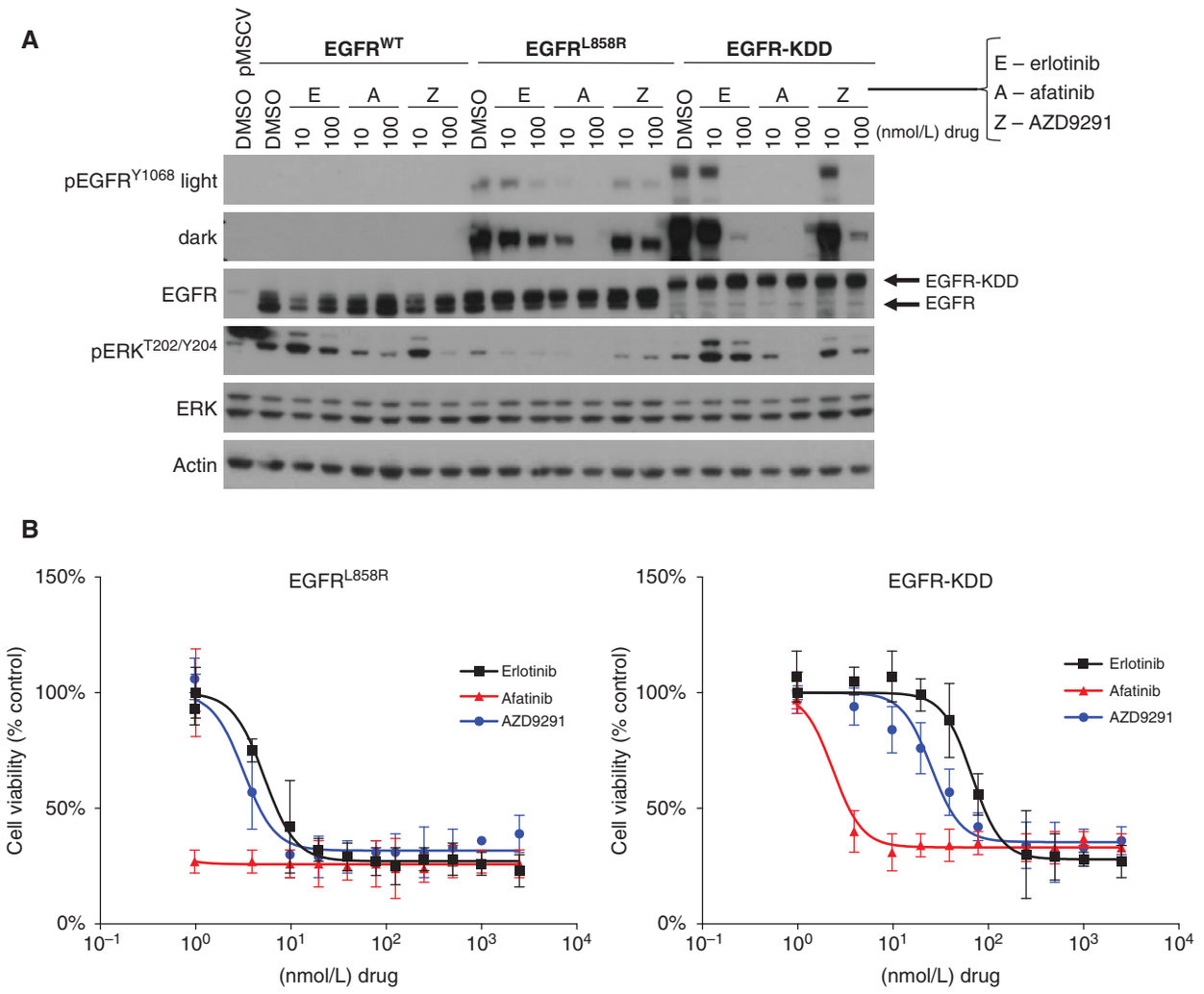

Figure 2. The EGFR-KDD can be therapeutically targeted with existing EGFR TKIs. **A,** Ba/F3 lines stably expressing EGFR^{WT}, EGFR^{L858R}, or EGFR-KDD were treated with increasing doses of erlotinib, afatinib, or AZD9291 for 2 hours and lysed for Western blot analysis with the indicated antibodies. **B,** Ba/F3 lines stably expressing EGFR^{L858R} or EGFR-KDD were treated with increasing doses of erlotinib, afatinib, or AZD9291 for 72 hours. Cell titer blue assays were performed to assess cell viability. Each point represents quadruplicate replicates. Data are presented as the mean percentage of viable cells compared with vehicle control ± SD.

time of disease progression on this treatment regimen, the patient was treated with afatinib. Immediately after beginning afatinib, the patient reported feeling markedly better, with improvements in his symptoms of cough and fatigue. After two cycles of afatinib, the patient showed a partial radiographic response (~50% tumor shrinkage) per RECIST criteria (ref. 17; Fig. 3A). This clinical activity is consistent with our *in vitro* studies and provides a rationale for further clinical investigation.

Acquired Resistance to Afatinib

The index patient developed acquired resistance to afatinib after 7 cycles of therapy (Fig. 3A). This duration of response is in line with the typical responses observed in other *EGFR*-mutant lung cancers treated with EGFR TKIs (1–3). Molecular profiling was performed on the afatinib-resistant tumor biopsy sample, and this testing uncovered significant amplification of the *EGFR*-KDD allele as the only genomic alteration that differed from his pretreatment tumor sample (Fig. 3B). This sequencing result was confirmed via *EGFR* FISH (Fig. 3C). Amplification of the mutant *EGFR* allele has been reported as a mechanism of acquired resistance in the context of canonical *EGFR* mutations (e.g., exon 19 deletion, L858R) in lung cancer (18). Therefore, amplification of the *EGFR*-KDD in this post-treatment sample suggests an EGFR-dependent mechanism of resistance, thereby further validating this *EGFR* alteration as a driver and therapeutic target in patients.

DISCUSSION

Although much progress has been made over the past several decades, lung cancer remains the leading cause of

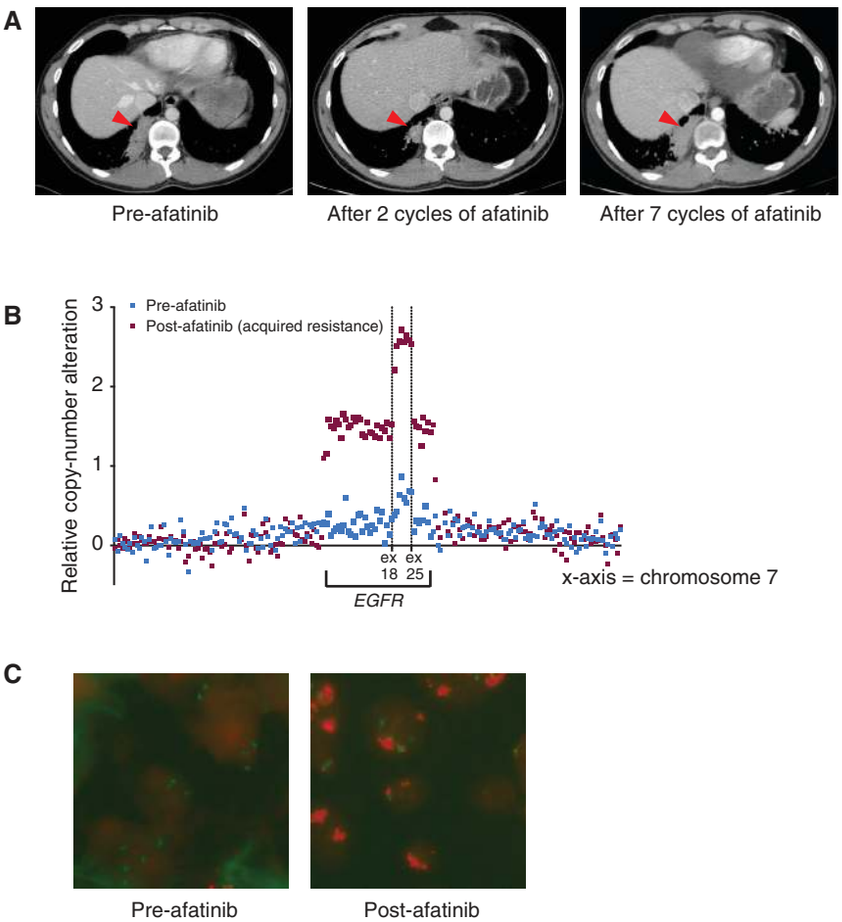

Figure 3. Serial chest CT scans of 33-year-old male with lung adenocarcinoma harboring *EGFR*-KDD documenting response to afatinib and subsequent acquired resistance. **A,** left image, patient images after six cycles of cisplatin/pemetrexed/bevacizumab (largest mass diameter = 6.62 cm). Middle image, patient images after two cycles of afatinib (largest mass diameter = 2.72 cm). Right image, patient images after seven cycles of afatinib (largest mass diameter = 6.20 cm). The red arrowheads are pointing to the largest mass used for RECIST evaluation. **B,** copy-number data from FoundationOne NGS targets along chromosome 7 demonstrating amplification of the *EGFR*-KDD allele at the time of acquired resistance to afatinib (maroon squares) compared with the pre-afatinib tumor biopsy sample (blue squares). The *x*-axis represents chromosome 7. **C,** *EGFR* FISH of pre-afatinib (left image) and post-afatinib (right image) tumor biopsy samples used for the NGS analysis shown in **B**. Pre-afatinib, 1.6 copies of *EGFR* per chromosome 7 centromere (1.6 *EGFR/CEP7*); post-afatinib, 4.2 *EGFR/CEP7*. Green puncta, *CEP7*; red puncta, *EGFR*.

cancer death worldwide (19). The discovery of oncogenic *EGFR* mutations that sensitize lung cancers to EGFR TKIs heralded the dawn of molecularly targeted therapy in this disease (20–22). Indeed, numerous phase III studies have now documented that patients with *EGFR*-mutant tumors derive significant clinical and radiographic benefit from treatment with EGFR TKIs, such as gefitinib, erlotinib, and afatinib (1–3). The majority of previously described activating mutations in *EGFR* are a series of small deletions in exon 19 or leucine-to-arginine substitutions at position 858 (L858R) in exon 21 (23). However, because mutations historically have been interrogated by "hot-spot" PCR-based methods, most *EGFR* mutations are biased to fall between exons 18 and 21.

Here, we report the *EGFR*-KDD for the first time in lung cancer. This *EGFR* alteration contains an in-tandem and in-frame duplication of exons 18 to 25, which encode the entire EGFR kinase domain. We demonstrate that the EGFR-KDD is an oncogenic and constitutively activated form of the EGFR. We provide a structural model whereby the EGFR-KDD can be activated by virtue of asymmetric intramolecular dimerization, as opposed to the typical asymmetric intermolecular dimerization between adjacent EGFR molecules. Furthermore, we demonstrate that the EGFR-KDD can be therapeutically targeted with EGFR TKIs, many of which are already FDA approved. In addition, we establish that the *EGFR*-KDD alteration is recurrent not only in lung cancer but also in gliomas and other tumor types.

Most importantly, we provide the first documentation of a clinical response to EGFR inhibitor therapy in a patient with lung cancer whose tumor harbored the *EGFR*-KDD alteration. In contrast with lung cancer patients with more common *EGFR* mutations (e.g., exon 19 deletion and L858R), prior to our study, there was no precedent to support the use of EGFR inhibitors in patients whose lung tumors harbor the *EGFR*-KDD alteration. Therefore, our patient was not eligible for first-line EGFR TKI therapy and was instead treated with platinum-based chemotherapy, the standard of care for metastatic lung adenocarcinoma (24). The index patient was treated with afatinib for second-line therapy because this agent is FDA approved for the treatment of *EGFR*-mutant NSCLC and because, interestingly, afatinib was consistently the most potent EGFR TKI against the EGFR-KDD across several different assays. This was not unexpected, as it has been shown that various EGFR mutations or truncations have differential sensitivity to EGFR TKIs due to nuanced structural differences (25). The marked tumor regression and improved functional status seen with afatinib therapy provides important clinical validation for the *EGFR*-KDD as an actionable alteration in lung cancer. Overall, the index patient derived a partial response to afatinib for 7 cycles, after

which there was progression of disease. His tumor was rebiopsied and found to contain amplification of the *EGFR*-KDD in this post-treatment sample—suggesting an EGFR-dependent mechanism of resistance and validating this *EGFR* alteration as a driver and therapeutic target in patients.

This case also reinforces the need to functionally validate and discern the therapeutic "actionability" of genomic alterations as increasingly sophisticated methods of NGS-based assays are being brought to the forefront of clinical diagnostics. Notably, the *EGFR*-KDD would not have been recognized by the "hot-spot" PCR-based methods for *EGFR* mutational analysis described above. Therefore, it is not surprising that this *EGFR* alteration had not previously been detected. In fact, the *EGFR*-KDD in the index patient's tumor was identified because of a fortuitous intronic breakpoint that lay close to the exonic probes of the NGS diagnostic assay (Supplementary Fig. S1A). Therefore, we hypothesize that the *EGFR*-KDD may have gone and may continue to go undetected in other tumors because standard (exomic) sequencing platforms do not target this particular alteration due to its large intragenic repeat and intronic breakpoint. Thus, although our data show that the *EGFR*-KDD is recurrent in multiple tumor types, this alteration would not be detected with currently approved PCR-based methods and is difficult to detect using standard exomic sequencing, consequently making our reported frequency a likely underestimate. Future design of tumor sequencing platforms should incorporate intronic probes for *EGFR* in order to more reliably detect the *EGFR*-KDD.

In summary, we have identified a recurrent, oncogenic, and drug-sensitive EGFR-KDD in a subset of patients with lung cancer, glioma, and other cancer types. Our findings provide a rationale for therapeutically targeting this unique subset of EGFR-KDD–driven tumors with EGFR tyrosine kinase inhibitors, many of which are already FDA approved. Therefore, findings from our studies are expected to be rapidly translated into the clinic as they provide a new avenue for precision medicine in these difficult-to-treat malignancies.

METHODS

Cell Culture

The human lung adenocarcinoma cell line, II-18, has been previously described and was verified to harbor the $EGFR^{L858R}$ mutation by cDNA sequencing (26). A1235 cells were a kind gift from Drs. R. Fenstermaker and M. Ciesielski (Roswell Park Cancer Institute, Buffalo, NY; ref. 7). The 293T cells were purchased from the ATCC. Ba/F3 cells were purchased from DSMZ. Plat-GP cells were purchased from CellBioLabs. NR6 cells were a kind gift from Dr. William Pao (27). II-18 and Ba/F3 cells were maintained in RPMI 1640 medium (Mediatech, Inc.). A1235, 293T, and NR6 cells were maintained in DMEM (Gibco). Media were supplemented with 10% heat-inactivated FBS (Atlanta Biologicals) and penicillin–streptomycin (Mediatech, Inc.) to final concentrations of 100 U/mL and 100 μg/mL, respectively. The Ba/F3 cell line was supplemented with 1 ng/mL murine IL3 (Gibco). The Plat-GP cell line was cultured in the presence of 1 μg/mL blasticidin (Gibco). All cell lines were maintained in a humidified incubator with 5% CO_2 at 37°C and routinely evaluated for *Mycoplasma* contamination. Besides verifying the status of *EGFR* mutations in cell lines, no additional cell line identification was performed.

Compounds

Erlotinib, afatinib, and AZD9291 were purchased from Selleck Chemicals.

EGFR Plasmid Construction

A cDNA encoding the EGFR-KDD (exon 18–25 tandem duplication) was synthesized by Life Technologies based on the consensus coding sequence (Supplementary Fig. S2). The pMSCV-puro vector backbone (Clontech) was used to construct all retroviruses. Assembly of pMSCV-puro-$EGFR^{WT}$ and pMSCV-puro-$EGFR^{L858R}$ was previously described (28). The *EGFR*-KDD was subcloned from the pMA synthesis vector (Life Technologies) into the *HpaI* site of pMSCV-puro using blunt end ligation. The pcDNA3.1 vector was used for transient expression experiments in 293T cells. Assembly of pcDNA-$EGFR^{WT}$ and pcDNA-$EGFR^{L858R}$ was previously described (22). *EGFR*-KDD was subcloned from the pMA synthesis vector (Life Technologies) into the pcDNA3.1/V5 vector (Life Technologies) using Gateway cloning (Life Technologies). All plasmids were sequence verified in the forward and reverse directions. *EGFR*-KDD-dead was constructed using multisite-directed mutagenesis (Agilent) of the catalytic lysines (K745 and K1096) to methionines using the following primer:

KM-F: 5′–AAAGTTAAAATTCCCGTCGCTATCATGGAATTAAGAGAAGCAAC–3′.

The plasmids were fully resequenced in each case to ensure that no additional mutations were introduced.

Ba/F3 and NR6 Cell Line Generation

The empty pMSCV-puro retroviral vector or pMSCV-puro vectors encoding EGFR ($EGFR^{WT}$, $EGFR^{L858R}$, EGFR-KDD, or EGFR-KDD-dead) were transfected, along with the envelope plasmid pCMV-VSV-G (CellBioLabs), into Plat-GP packaging cells (CellBioLabs). Viral media were harvested 48 hours after transfection, spun down to remove debris, and supplemented with 2 μg/mL polybrene (Santa Cruz Technology). A total of 2.5×10^6 Ba/F3 cells (or 1×10^6 NR6 cells) were resuspended in 10 mL viral media. Transduced cells were selected for 1 week in 2 μg/mL puromycin (Invitrogen), and Ba/F3 cells were selected for an additional week in the absence of IL3. Stable polyclonal populations were used for experiments and routinely tested for expression of EGFR constructs.

Antibodies and Immunoblotting

The following antibodies were obtained from Cell Signaling Technology: phospho-EGFR tyrosine 1068 (#2234, 1:1,000 dilution), EGFR (#4267, 1:1,250 dilution), phospho-ERK threonine 202/tyrosine 204 (#9101, 1:2,000 dilution), ERK (#9102, 1:2,000 dilution), horseradish peroxidase (HRP)–conjugated anti-mouse (#7076, 1:5,000 dilution), and HRP-conjugated anti-rabbit (#7074, 1:5,000 dilution). The actin antibody (#A2066, 1:5,000 dilution) was purchased from Sigma-Aldrich. The EGFR antibody (#610017, 1:2,000 dilution) was purchased from BD Pharmingen. For immunoblotting, cells were harvested, washed in PBS, and lysed in RIPA buffer (150 mmol/L NaCl, 1% Triton-X-100, 0.5% Na-deoxycholate, 0.1% SDS, 50 mmol/L Tris·HCl, pH 8.0) with freshly added 40 mmol/L NaF, 1 mmol/L Na-orthovanadate, and protease inhibitor mini tablets (Thermo Scientific). Protein was quantified using protein assay reagent and a SmartSpec Plus spectrophotometer (Bio-Rad) per the manufacturer's protocol. Lysates were subjected to SDS-PAGE followed by blotting with the indicated antibodies and detection by Western Lightning ECL reagent (Perkin Elmer).

Cell Viability, Counting, and Clonogenic Assays

For viability experiments, cells were seeded at 5,000 cells/well in 96-well plates and exposed to treatment the following day. At 72 hours after drug addition, Cell Titer Blue reagent (Promega) was

added, and fluorescence at 570 nm was measured on a Synergy MX microplate reader (Biotek) according to the manufacturer's instructions. For cell counting experiments, cells were seeded at 20,000 cells/well in 24-well plates in the presence or absence of 1 ng/mL IL3. Every 24 hours, cells were diluted 20-fold and counted using a Z1 Coulter Counter (Danaher). For clonogenic assays, cells were seeded at 5,000 cells/well in 24-well plates and exposed to treatment the following day. Media and inhibitors were refreshed every 72 hours, and cells were grown for 1 week or until confluence in control wells. Cells were fixed with 4% v/v formalin and stained with 0.025% crystal violet. Dye intensity was quantified using an infrared imaging system (LI-COR). Viability assays were set up in quadruplicate, clonogenic assays were set up in triplicate, and cell-counting assays were set up in duplicate. All experiments were performed at least three independent times. Data are presented as the percentage of viable cells compared with control (vehicle only treated) cells. Regressions were generated as sigmoidal dose–response curves using Prism 6 (GraphPad) by normalizing data and constraining the top to 100.

Soft-Agar Assays

1.5 mL of 0.5% agar/DMEM was layered in each well of a 6-well dish. A total of 10,000 NR6 cells in 1.5 mL of 0.33% soft agar/DMEM were seeded on top of the initial agar and allowed to grow for 15 days. Each cell line was plated in triplicate. Colonies were counted using GelCount (Oxford Optronix) with identical acquisition and analysis settings.

Transient Transfections

The 293T cells were transfected using Lipofectamine 2000 (Life Technologies) per the manufacturer's recommendations. Twenty-four hours after transfection, cells were treated for 2 hours, gathered for Western blot analysis, and prepared as described above.

Structural Modeling of the EGFR-KDD

The linker residues in the EGFR-KDD protein sequence, FFSSPSTSRTPLLSSLLVEPLTPS, were defined as those between the two kinase domains and not present in the X-ray crystal structure of EGFR in its allosterically activated dimeric form, 2GS6.pdb (13). This linker was manually built and placed into the EGFR crystal structure using PyMOL 1.5.0.3. The conformational space for the linker was then sampled using the loop-modeling functionality of Rosetta version 2015.05 (29). A total of 20,000 independent loop modeling runs were performed using kinematic closure. The best model from these runs was still lacking residues 748–750, 992–1004, 1099–1101, and 1343–1355 because these surface-exposed loops were not resolved in the experimental structure. These four loops were reconstructed using Modeller 9.14, and the model with the lowest DOPE score was selected (30). Those loops were then sampled for an additional 20,000 runs using Rosetta to generate the complete energy-minimized model of EGFR-KDD residues GLY 696 - PRO 1370.

Tumor Biopsy Samples

All patient tumor biopsy samples were obtained under Institutional Review Board (IRB)–approved protocols (Vanderbilt University IRB# 050644). Written informed consent was obtained from the index patient. All samples were deidentified, protected health information reviewed according to the Health Insurance Portability and Accountability Act (HIPAA) guidelines, and studies conducted in accordance with the Declaration of Helsinki.

Identifying EGFR-KDD in The Cancer Genome Atlas

Copy-number data from the Broad Institute TCGA Genome Data Analysis Center 2015-04-02 run were visually inspected to identify samples with focal amplification of the *EGFR*-KDD region (exons 18–25). RNA sequencing (e714b8a4-dd57-4b01-83fd-d3a9fb2d4ad1120 and c552b1e3-9158-4c4d-b02b-b16ff7903552) and whole-genome sequencing (27c2031a-39f1-473c-88a6-9e7a03cedf04) files were inspected to confirm the presence of tandem duplication reads. Raw data were available at doi:10.7908/C1K64H04 and doi:10.7908/C1MP525H.

EGFR FISH

EGFR FISH was performed by Integrated Oncology, a LabCorp specialty testing group, using the *EGFR-CEP7* Dual Color DNA Probe (Vysis). A trained pathologist quantified the copies of *CEP7* and *EGFR* in 60 nuclei per sample.

Statistics and Data Presentation

All experiments were performed using at least two technical replicates and at least three independent times (biologic replicates). Each figure or panel shows a single representative experiment. Unless indicated otherwise, data are presented as mean ± SD. Western blot autoradiography films were scanned in full color at 600 dpi, desaturated in Adobe Photoshop CC, and cropped in Powerpoint. *EGFR*-FISH images were normalized using "Match Color" in Adobe Photoshop CC. No other image alterations were made.

Disclosure of Potential Conflicts of Interest

M. Bailey has ownership interest (including patents) in Foundation Medicine Inc. D. Lipson has ownership interest (including patents) in Foundation Medicine Inc. M.G. Kris reports receiving commercial research grants from Pfizer and PUMA, and is a consultant/advisory board member for AstraZeneca and Roche/Genentech. V.A. Miller has ownership interest (including patents) in Foundation Medicine. S.M. Ali has ownership interest (including patents) in Foundation Medicine. C.M. Lovly reports receiving commercial research grants from AstraZeneca and Novartis; has received speakers bureau honoraria from Abbott Molecular and Qiagen; and is a consultant/advisory board member for Genoptix, Novartis, Pfizer, and Sequenom. No potential conflicts of interest were disclosed by the other authors.

Authors' Contributions

Conception and design: J.-N. Gallant, J. Meiler, C.M. Lovly
Development of methodology: J.-N. Gallant, D. Lipson, J. Meiler, C.M. Lovly
Acquisition of data (provided animals, acquired and managed patients, provided facilities, etc.): J.-N. Gallant, T.M. Shaver, M.G. Kris, J.A. Pietenpol, M. Ladanyi, V.A. Miller, S.M. Ali, C.M. Lovly
Analysis and interpretation of data (e.g., statistical analysis, biostatistics, computational analysis): J.-N. Gallant, J.H. Sheehan, T.M. Shaver, M. Bailey, D. Lipson, R. Chandramohan, M.R. Brewer, M.G. Kris, J.A. Pietenpol, J. Meiler, C.M. Lovly
Writing, review, and/or revision of the manuscript: J.-N. Gallant, J.H. Sheehan, M.R. Brewer, M.G. Kris, J.A. Pietenpol, M. Ladanyi, V.A. Miller, S.M. Ali, J. Meiler, C.M. Lovly
Administrative, technical, or material support (i.e., reporting or organizing data, constructing databases): M.G. Kris, J.A. Pietenpol, C.M. Lovly
Study supervision: M.G. Kris, J. Meiler, C.M. Lovly
Other (involved in the initial description of the mutation, discussed experimental results with the senior author, and provided clinical care for the patient described in the study): S.J. York
Other (coordinated studies): J.-N. Gallant

Acknowledgments

The authors thank the index patient and his family. They also thank Evelyn Vazquez for her assistance with the *EGFR* FISH.

Grant Support

This study was supported in part by the NIH and NCI R01CA121210 (to C.M. Lovly), P01CA129243 (to C.M. Lovly, M. Ladanyi, and M.G. Kris),

and P30CA68485. Work in the Meiler laboratory is supported through the NIH (R01GM080403, R01GM099842, R01DK097376, R01HL122010, and R01GM073151) and the NSF (CHE1305874). C.M. Lovly was additionally supported by a Damon Runyon Clinical Investigator Award and a LUNGevity Career Development Award. J.-N. Gallant was supported by MSTP grant T32GM007347. T.M. Shaver was supported by F31CA183531.

The costs of publication of this article were defrayed in part by the payment of page charges. This article must therefore be hereby marked *advertisement* in accordance with 18 U.S.C. Section 1734 solely to indicate this fact.

Received May 28, 2015; revised August 12, 2015; accepted August 13, 2015; published OnlineFirst August 18, 2015.

REFERENCES

1. Mok TS, Wu Y-L, Thongprasert S, Yang C-H, Chu D-T, Saijo N, et al. Gefitinib or carboplatin-paclitaxel in pulmonary adenocarcinoma. N Engl J Med 2009;361:947–57.
2. Rosell R, Carcereny E, Gervais R, Vergnenegre A, Massuti B, Felip E, et al. Erlotinib versus standard chemotherapy as first-line treatment for European patients with advanced EGFR mutation-positive non-small-cell lung cancer (EURTAC): a multicentre, open-label, randomised phase 3 trial. Lancet Oncol 2012;13:239–46.
3. Sequist LV, Yang JC-H, Yamamoto N, O'Byrne K, Hirsh V, Mok T, et al. Phase III study of afatinib or cisplatin plus pemetrexed in patients with metastatic lung adenocarcinoma with EGFR mutations. J Clin Oncol 2013;31:3327–34.
4. Carey KD, Garton AJ, Romero MS, Kahler J, Thomson S, Ross S, et al. Kinetic analysis of epidermal growth factor receptor somatic mutant proteins shows increased sensitivity to the epidermal growth factor receptor tyrosine kinase inhibitor, erlotinib. Cancer Res 2006; 66:8163–71.
5. Frampton GM, Fichtenholtz A, Otto GA, Wang K, Downing SR, He J, et al. Development and validation of a clinical cancer genomic profiling test based on massively parallel DNA sequencing. Nat Biotechnol 2013;31:1023–31.
6. Cheng DT, Mitchell TN, Zehir A, Shah RH, Benayed R, Syed A, et al. Memorial Sloan Kettering-integrated mutation profiling of actionable cancer targets (MSK-IMPACT): a hybridization capture-based next-generation sequencing clinical assay for solid tumor molecular oncology. J Mol Diagn 2015;17:251–64.
7. Fenstermaker RA, Ciesielski MJ, Castiglia GJ. Tandem duplication of the epidermal growth factor receptor tyrosine kinase and calcium internalization domains in A-172 glioma cells. Oncogene 1998;16: 3435–43.
8. Ciesielski MJ, Fenstermaker RA. Oncogenic epidermal growth factor receptor mutants with tandem duplication: gene structure and effects on receptor function. Oncogene 2000;19:810–20.
9. Frederick L, Wang XY, Eley G, James CD. Diversity and frequency of epidermal growth factor receptor mutations in human glioblastomas. Cancer Res 2000;60:1383–7.
10. Ozer BH, Wiepz GJ, Bertics PJ. Activity and cellular localization of an oncogenic glioblastoma multiforme- associated EGF receptor mutant possessing a duplicated kinase domain. Oncogene 2009;29:855–64.
11. Furgason JM, Li W, Milholland B, Cross E, Li Y, McPherson CM, et al. Whole genome sequencing of glioblastoma multiforme identifies multiple structural variations involved in EGFR activation. Mutagenesis 2014;29:341–50.
12. Greulich H, Chen T-H, Feng W, Jänne PA, Alvarez JV, Zappaterra M, et al. Oncogenic transformation by inhibitor-sensitive and -resistant EGFR mutants. PLoS Med 2005;2:e313.
13. Zhang X, Gureasko J, Shen K, Cole PA, Kuriyan J. An allosteric mechanism for activation of the kinase domain of epidermal growth factor receptor. Cell 2006;125:1137–49.
14. Moyer JD, Barbacci EG, Iwata KK, Arnold L, Boman B, Cunningham A, et al. Induction of apoptosis and cell cycle arrest by CP-358,774, an inhibitor of epidermal growth factor receptor tyrosine kinase. Cancer Res 1997;57:4838–48.
15. Li D, Ambrogio L, Shimamura T, Kubo S, Takahashi M, Chirieac LR, et al. BIBW2992, an irreversible EGFR/HER2 inhibitor highly effective in preclinical lung cancer models. Oncogene 2008;27:4702–11.
16. Cross DAE, Ashton SE, Ghiorghiu S, Eberlein C, Nebhan CA, Spitzler PJ, et al. AZD9291, an irreversible EGFR TKI, overcomes T790M-mediated resistance to EGFR inhibitors in lung cancer. Cancer Discov 2014;4:1046–61.
17. Eisenhauer EA, Therasse P, Bogaerts J, Schwartz LH, Sargent D, Ford R, et al. New response evaluation criteria in solid tumours: revised RECIST guideline (version 1.1). Eur J Cancer 2009;45:228–47.
18. Sequist LV, Waltman BA, Dias-Santagata D, Digumarthy S, Turke AB, Fidias P, et al. Genotypic and histological evolution of lung cancers acquiring resistance to EGFR inhibitors. Sci Transl Med 2011;3: 75ra26–6.
19. Siegel RL, Miller KD, Jemal A. Cancer statistics, 2015. CA Cancer J Clin 2015;65:5–29.
20. Paez JG, Jänne PA, Lee JC, Tracy S, Greulich H, Gabriel S, et al. EGFR mutations in lung cancer: correlation with clinical response to gefitinib therapy. Science 2004;304:1497–500.
21. Lynch TJ, Bell DW, Sordella R, Gurubhagavatula S, Okimoto RA, Brannigan BW, et al. Activating mutations in the epidermal growth factor receptor underlying responsiveness of non-small-cell lung cancer to gefitinib. N Engl J Med 2004;350:2129–39.
22. Pao W, Miller V, Zakowski M, Doherty J, Politi K, Sarkaria I, et al. EGF receptor gene mutations are common in lung cancers from "never smokers" and are associated with sensitivity of tumors to gefitinib and erlotinib. Proc Natl Acad Sci U S A 2004;101:13306–11.
23. Forbes SA, Beare D, Gunasekaran P, Leung K, Bindal N, Boutselakis H, et al. COSMIC: exploring the world's knowledge of somatic mutations in human cancer. Nucleic Acids Res 2015;43:D805–11.
24. Ettinger DS, Wood DE, Akerley W, Bazhenova LA, Borghaei H, Camidge DR, et al. Non-small cell lung cancer, version 6.2015. J Natl Compr Canc Netw 2015;13:515–24.
25. Vivanco I, Robins HI, Rohle D, Campos C, Grommes C, Nghiemphu PL, et al. Differential sensitivity of glioma- versus lung cancer-specific EGFR mutations to EGFR kinase inhibitors. Cancer Discov 2012;2: 458–71.
26. Ohashi K, Sequist LV, Arcila ME, Moran T, Chmielecki J, Lin Y-L, et al. Lung cancers with acquired resistance to EGFR inhibitors occasionally harbor BRAF gene mutations but lack mutations in KRAS, NRAS, or MEK1. Proc Natl Acad Sci U S A 2012;109:E2127–33.
27. Regales L, Gong Y, Shen R, de Stanchina E, Vivanco I, Goel A, et al. Dual targeting of EGFR can overcome a major drug resistance mutation in mouse models of EGFR mutant lung cancer. J Clin Invest 2009;119:3000–10.
28. Red Brewer M, Yun C-H, Lai D, Lemmon MA, Eck MJ, Pao W. Mechanism for activation of mutated epidermal growth factor receptors in lung cancer. Proc Natl Acad Sci U S A 2013;110:E3595–604.
29. Stein A, Kortemme T. Improvements to robotics-inspired conformational sampling in Rosetta. PLoS ONE 2013;8:e63090.
30. Eswar N, Eramian D, Webb B, Shen M-Y, Sali A. Protein structure modeling with MODELLER. Methods Mol Biol 2008;426:145–59.